Flux pinning mechanism and RF properties of ingot Niobium used in SRF cavity fabrication

Pashupati Dhakal

09/26/2011

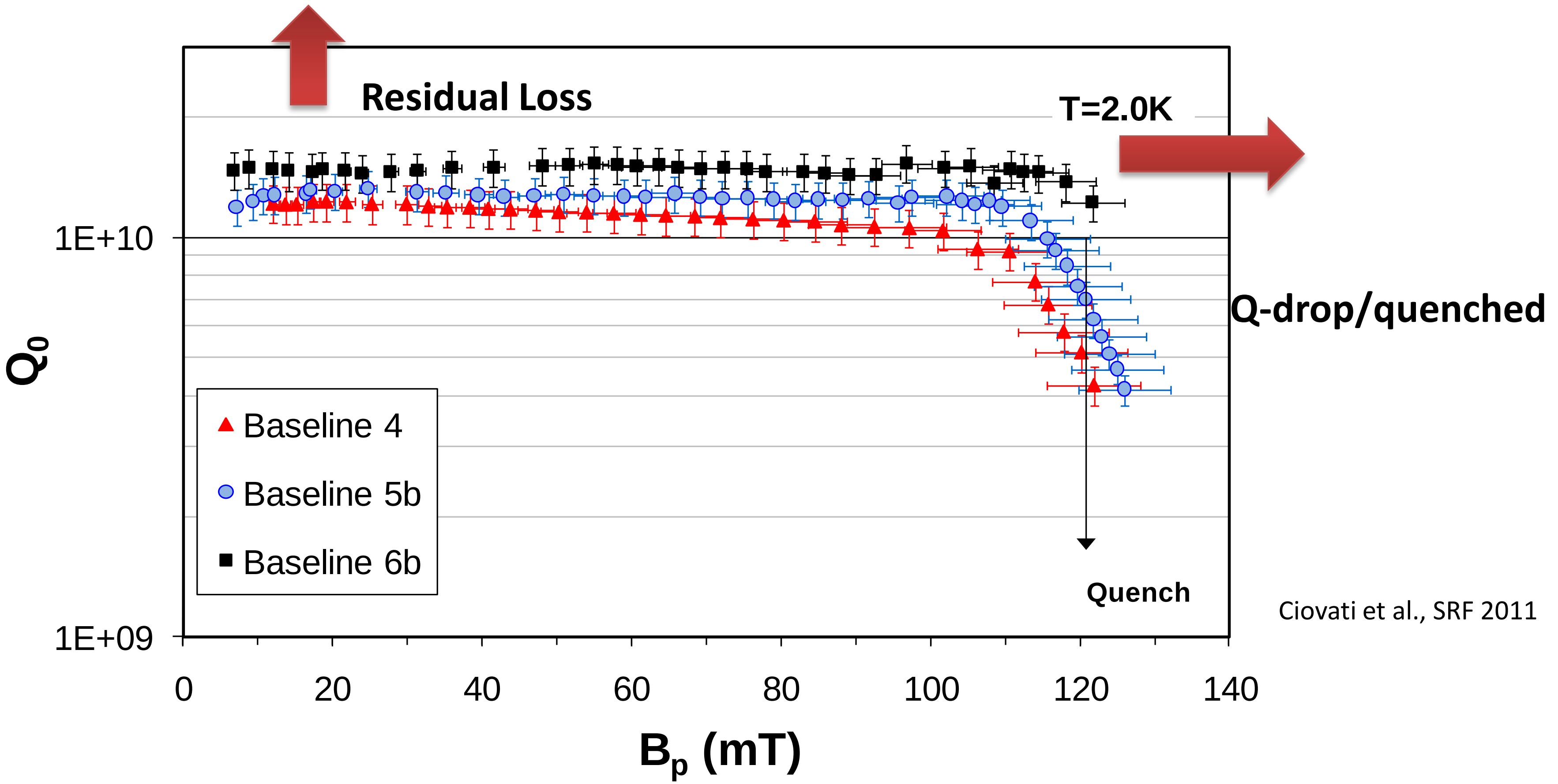

Higher Q_0 for the reduction of cryogenic loss
Higher E_{acc} for the use of high energy accelerators

Residual Loss

Magnetic vortices trapped at the surface of SRF Nb cavities are a well-known source of RF residual losses.

1. Vortices pinned near the surface oscillate under the Lorentz force given by the RF field
2. At higher field the vortices oscillates and propagates into the materials, resulting the increase in surface resistance.

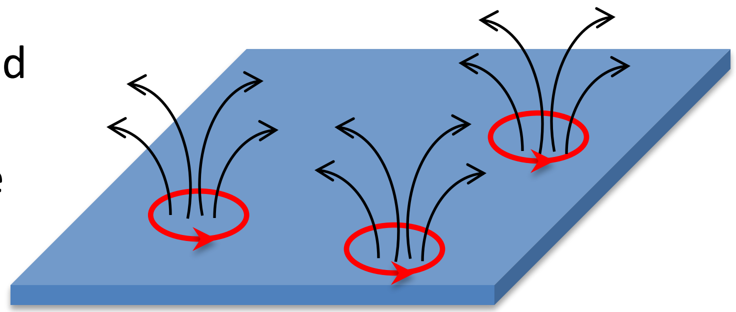

Magnetic Vortices can be produced due to

- **Imperfect shielding of the Earth's magnetic field**
- **thermoelectric currents during cavity cool down across the critical temperature**

Magnetic flux can be pinned in material defects, such as grain boundaries, dislocations or clusters of impurities

Experiments are in progress to remove the magnetic vortices pinned near the surface by means of heat.

Ciovati et al., SRF 2011

High-field Q slope

- Improvement for the Q drop had already been found (100–140C, 24-48 hrs) baking of the cavities in ultrahigh vacuum.
- Model based on “thermal diffusion” by A. Gurevich and “field dependent surface resistance” on defects sites by Weingarten qualitatively reproduce the experimental data.

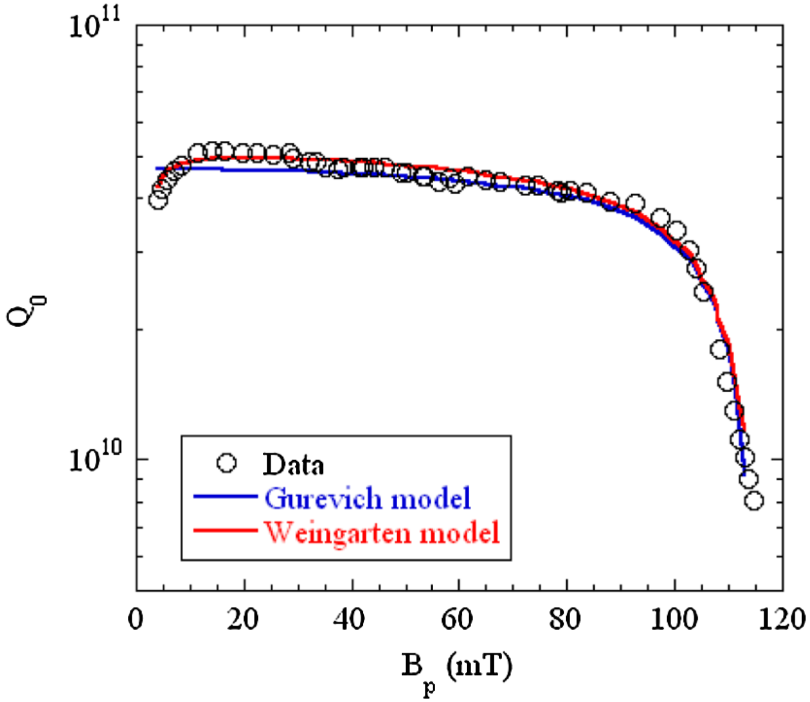

Ciovati et al., PRST- AB 13, 022002 (2010)

Motivations

✍ **Understanding the flux-pinning mechanisms and trapping efficiency in Nb material of different grain size and purity is important for the fabrication of SRF cavities with high quality factor.**

✍ **Effect of surface and heat treatments on RF properties on sample rods.**

Review

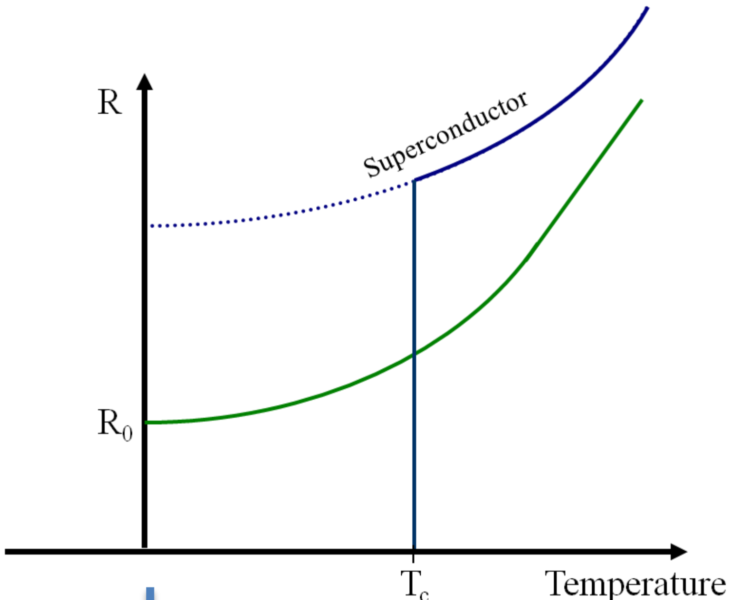

Meissner Effect

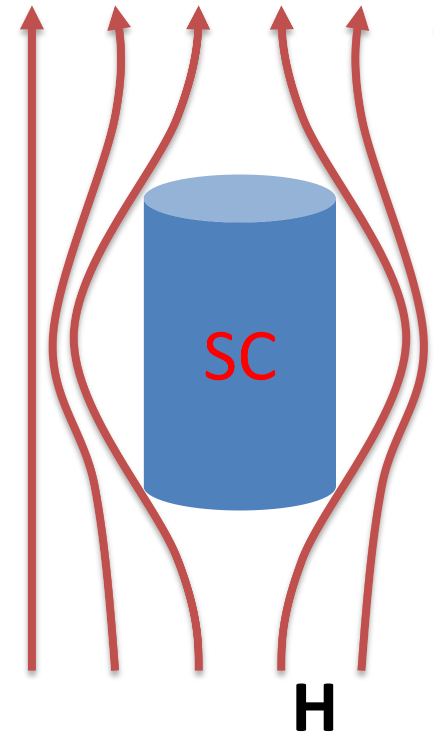

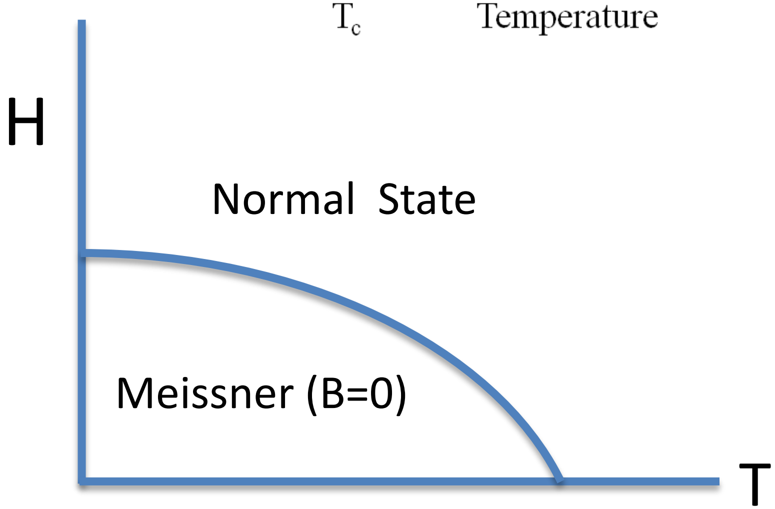

Type-I

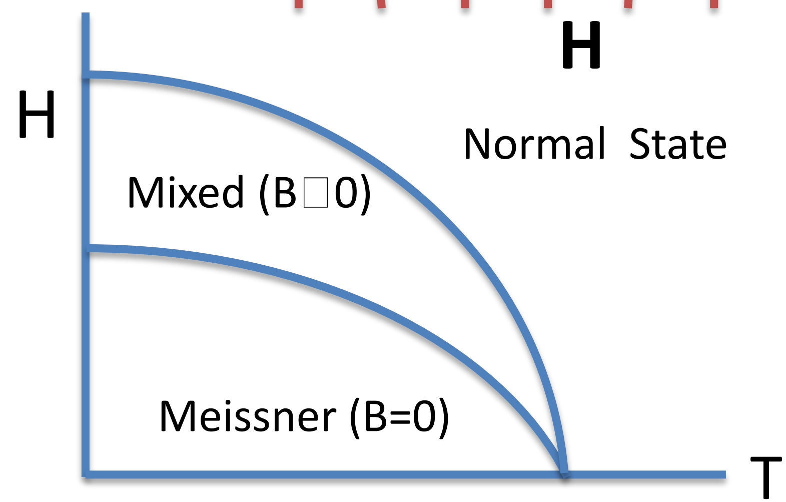

Type-II

Type-I vs Type-II Magnetization

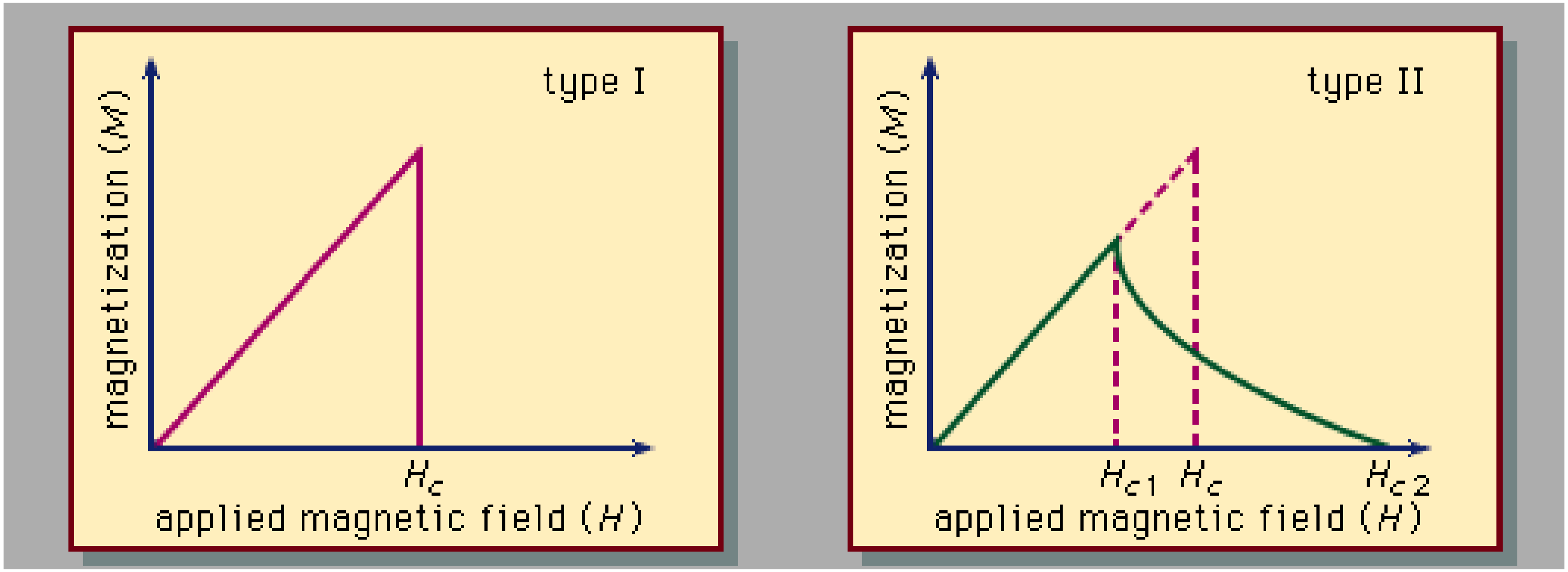

Niobium

Tc = 9.25 K

H_{c1} □170 mT

H_{c2} □ 420 mT

H_c □ 190 mT

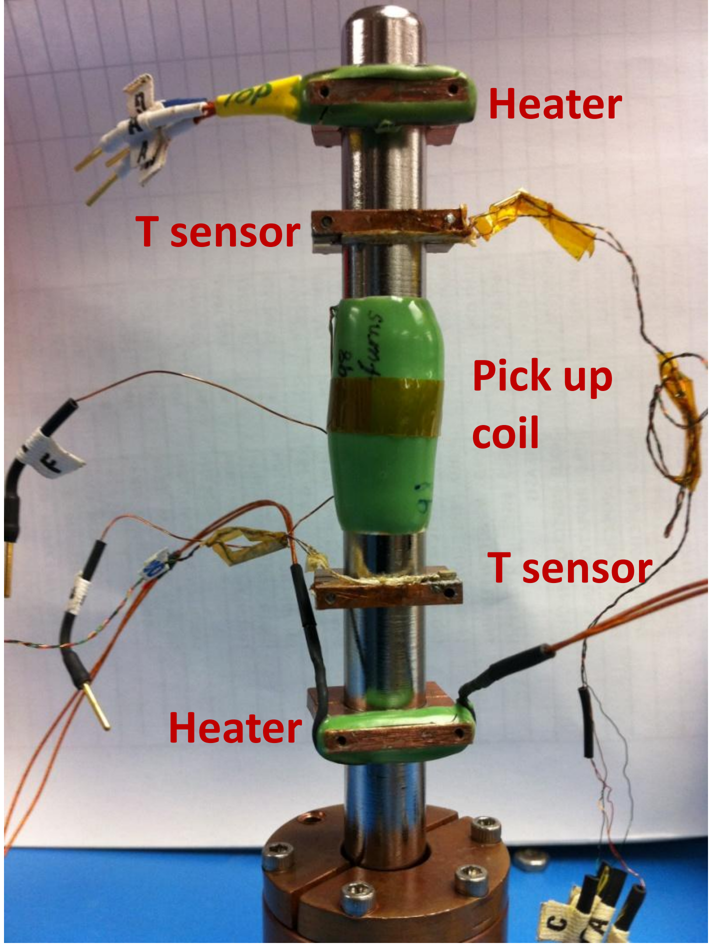

Experimental Set up

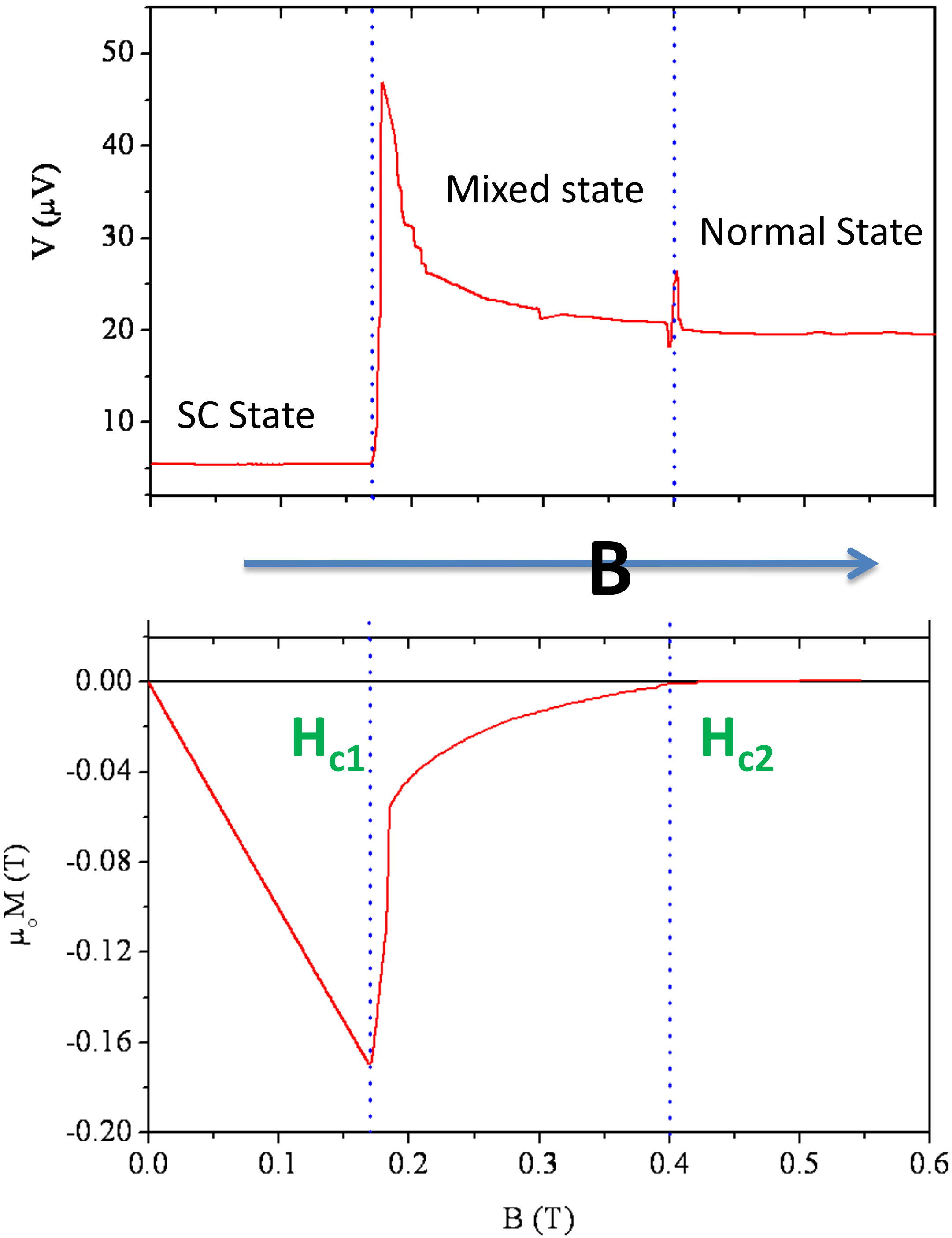

Magnetization is Given by

$$M(H_e) = \left(\frac{-1}{1 - N_d} \right) \int_0^{H_{dc}} \frac{V(H') - V_n}{V_s - V_n} \, dH'$$

Sample Preparation

Previously *Mondal et al., SRF 2009*

•LG (4 Samples)

- About 180 μm BCP
- Heat treatment at 600 °C/10 hrs in a UHV furnace
- ~ 24 μm BCP
- Baking in UHV at 100°C/12hrs, 120 °C/12hrs, 140 °C/12hrs and 160 °C/12hrs. About 10 μm were etched by BCP after each bake.

FG

- ~65 μm BCP
- Heat treatment at 800 °C/2 hrs in a UHV furnace
- ~ 140 μm BCP
- Heat treatment at 600 °C/10 hrs in a UHV furnace
- Post-purification heat treatment at 1250 °C for 3 hrs using Ti as solid state getter
- ~ 100 μm BCP

Now

- 50 μm material removal by electropolishing (EP) with $HF:H_2SO_4 = 1:10$ acid mixture.
- Baking in UHV at 120 °C/48 h (LTB)

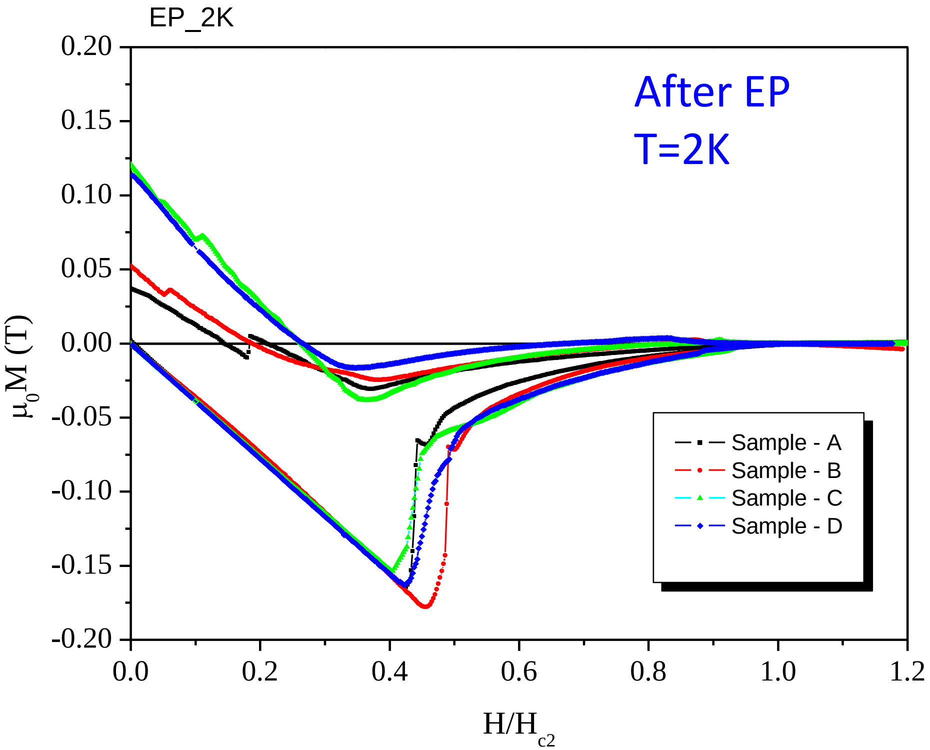

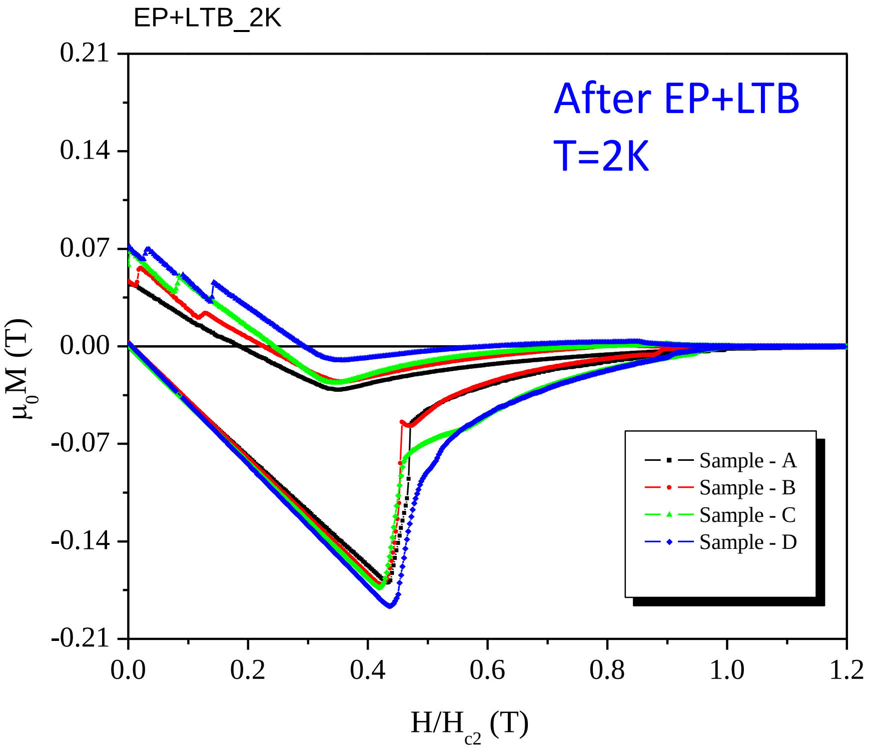

Sample	*Ta (ppm)*	*H (ppm)*	*C (ppm)*	*O (ppm)*	*N (ppm)*	*RRR*
A	1295	2	<10	21	10	62
B	1310	2	<10	9	3	164
C	603	4	<10	14	9	159
D	644	3	<10	7	7	118
FG	<100	<3	<20	<40	<20	280

Magnetization shows the same behavior irrespective to the impurities

LTB doesn't affect the bulk properties

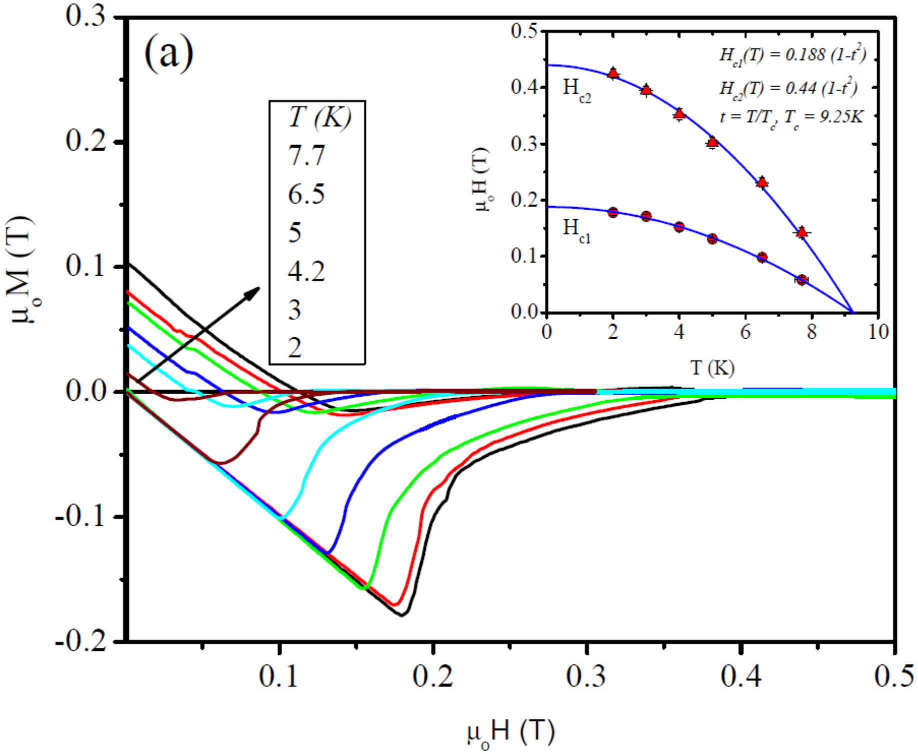

Sample-D (EP)

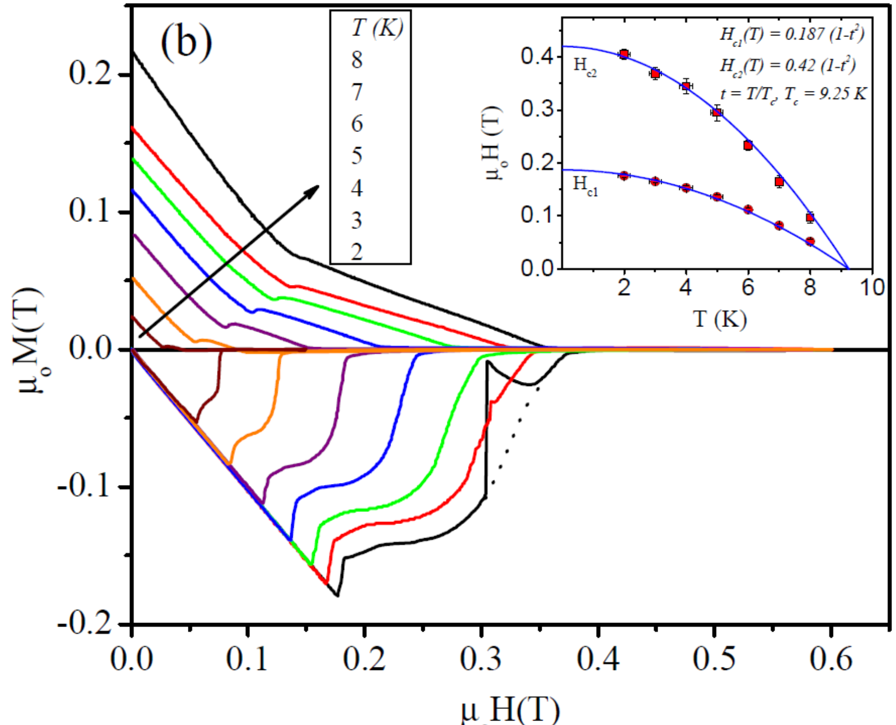

Sample-FG (EP)

Sample	EP			EP+LTB (120 ºC for 48 hrs)		
	$\mu_0 H_{ffp}(0)$ (mT)	$\mu_0 H_{c2}(0)$ (mT)	T_c (K)	$\mu_0 H_{ffp}(0)$ (mT)	$\mu_0 H_{c2}(0)$ (mT)	T_c (K)
A	187±4	418±8	9.25±0.01	190±7	427±8	9.22±0.02
B	183±3	411±10	9.12±0.02	185±4	421±8	9.26±0.02
C	194±5	443±11	9.21±0.02	193±11	445±12	9.24±0.01
D	188±5	440±10	9.21±0.03	192±9	439±11	9.24±0.02
FG	187±3	420±8	9.34±0.04	191±10	420±7	9.27±0.03

Measured bulk properties are average and hence not sensitive to surface treatments.

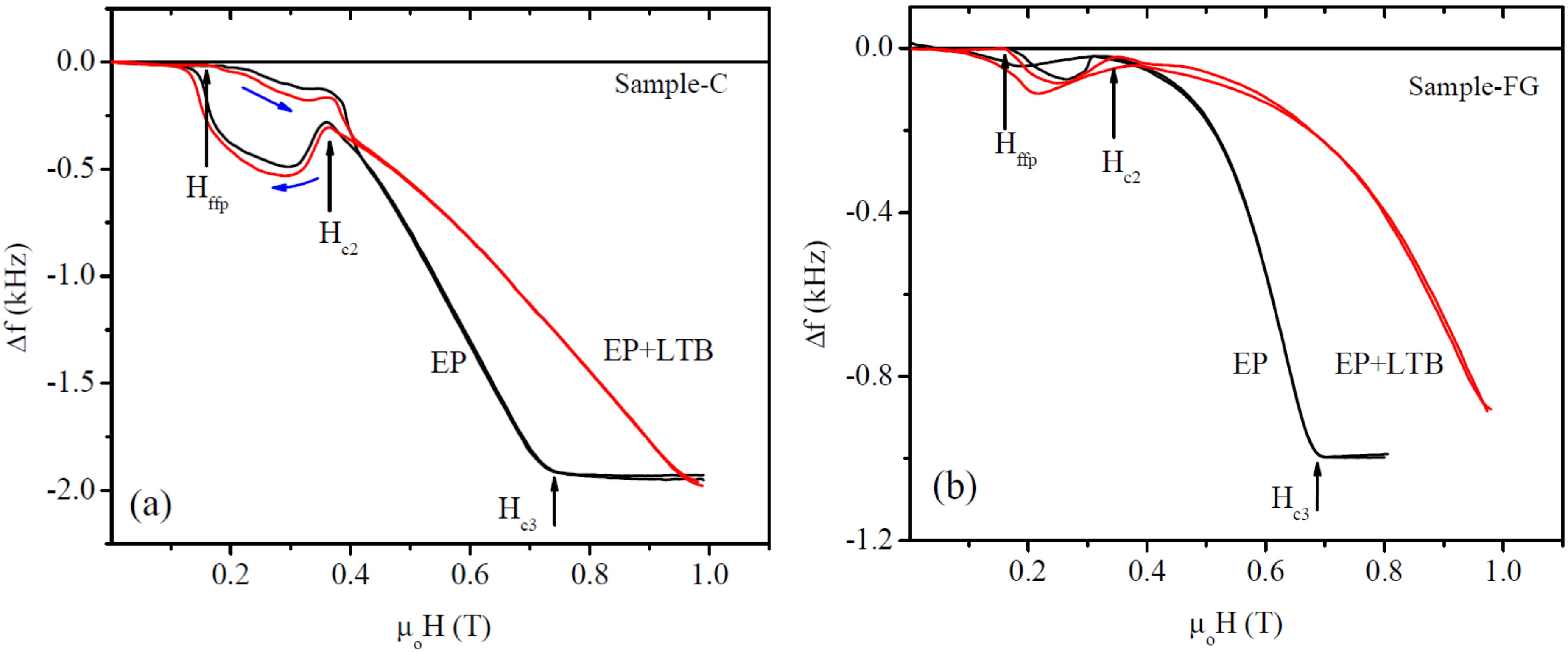

Samples	EP			EP+LTB (120 ºC for 48 hrs)		
	$\mu_0 H_{ffp}$ (mT)	$\mu_0 H_{c2}$ (mT)	$\mu_0 H_{c3}$ (mT)	$\mu_0 H_{ffp}$ (mT)	$\mu_0 H_{c2}$ (mT)	$\mu_0 H_{c3}$ (mT)
A	178±10	384±10	736±15	173±7	373±11	766±12
B	170±6	336±7	705±12	173±7	365±10	>1000
C	160±8	333±6	753±10	165 ±6	353±9	~1000
D	165±7	345±6	710±13	166±6	347±9	745±12
FG	168±10	358±9	689±15	171±5	362±8	>1000

Reduction of the electron mean free path takes place due to the diffusion of impurities during LTB.

LTB enhance the surface critical field H_{c3} and hence the ratio H_{c3}/H_{c2}.

Critical State

Once flux penetrates static magnetic flux distribution is determined by the balance between the Lorentz force and pinning force

$$F_p = J_c \times B$$

Critical State Models

$$J(B) = J_c \qquad \textit{Bean}$$

$$J(B) = \frac{J_c}{B(x)/B_o} \qquad \textit{Fixed Pinning (Ji et al, 1989)}$$

$$J(B) = \frac{J_c}{\left(B(x)/B_o\right)^{1/2}} \qquad \textit{Square Root (Le Blanc and Le Blanc, 1992)}$$

$$J(B) = \frac{J_c}{1 + B(x)/B_o} \qquad \textit{Kim et al., 1962}$$

$$J(B) = J_c \exp[-B(x)/B_o] \qquad \textit{Fietz et al, 1964}$$

$$J(B) = J_c - \frac{J_c B(x)}{B_o} \qquad \textit{Linear, Watson 1968}$$

Many More

In all these models, the magnetic field and the current density are coupled through the Maxwell relations $\nabla \times B = \mu_0 J$

These models don't really explains the nature of superconductivity but provide the convenient means of describing some experimentally observed phenomena.

Static magnetic flux distribution is determined by the balance between the Lorentz force and pinning force

$$\mathbf{F_p = J_c \times B}$$

Experimentally, Critical current can be calculated from magnetization measurements as

$$J_c(B) = \frac{3}{2}\Delta M(B)\left(\frac{R_{out}^{\,2} - R_{in}^{\,2}}{R_{out}^{\,3} - R_{in}^{\,3}}\right)$$

(widely used Bean model)

Even though the Bean model successfully explained the critical state of high *k* type-II superconductor, it deviates for the low *k* and weakly pinned superconductors where the diamagnetic contribution to critical state is significant.

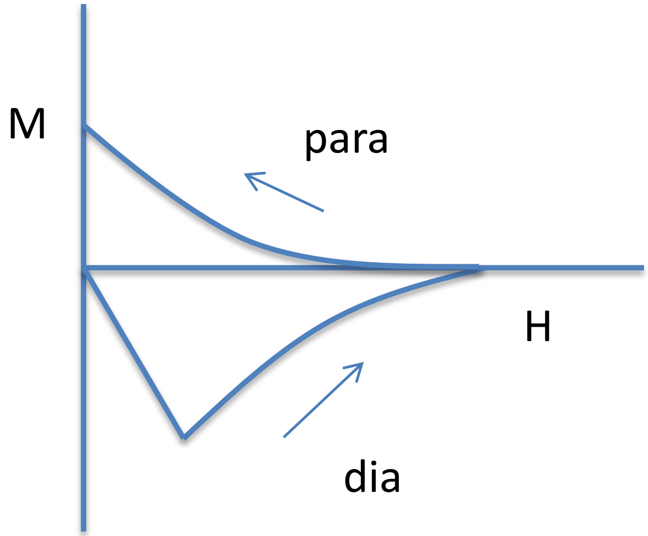

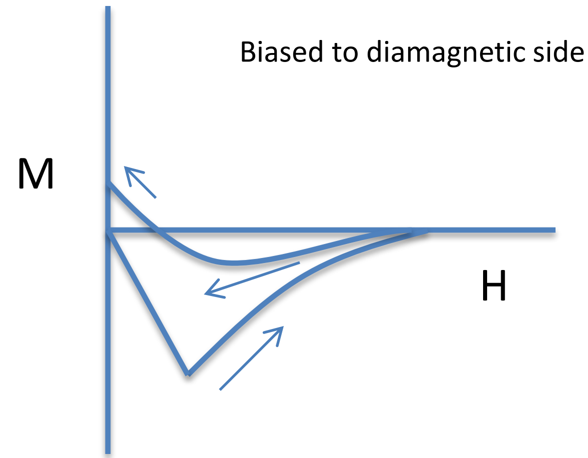

Diamagnetic magnetization is much smaller than the magnetization due to pinning effect

Effect of diamagnetism can't be neglected

1. For small κ
2. For which pinning force is weak
3. Small sized superconductor

The magnetization due to pinning is large in case where diamagnetism is small, critical current density is large, and superconductor is large in size

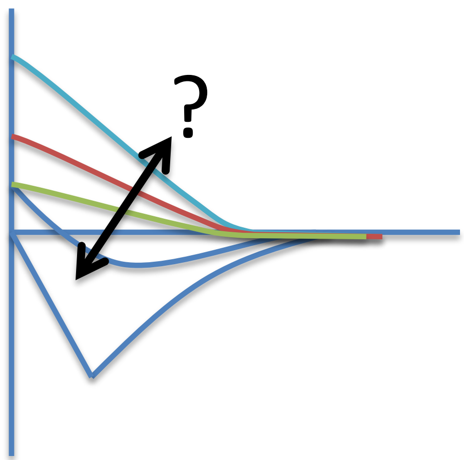

LG vs FG (shape of M-H Curve)

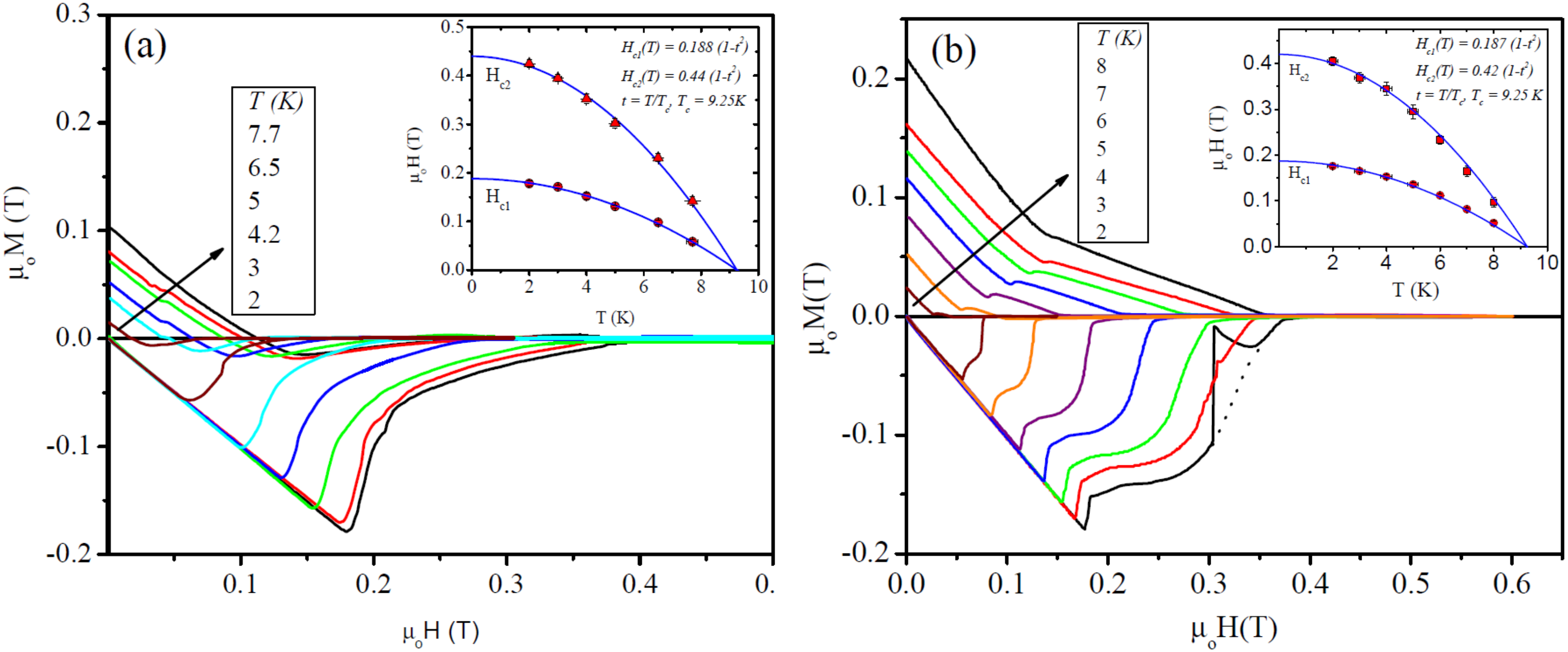

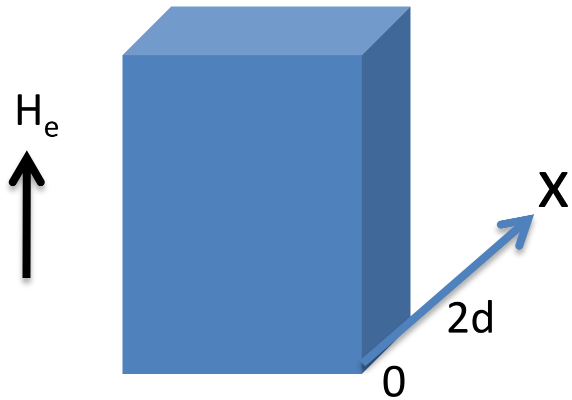

For Initial Magnetization, Increasing field

$0<H_e<H_{c1}$ → No flux line exists (Meissner State) and B = 0, H = 0

$H_e > H_{c1}$ → Field penetrates sample and B and H exist

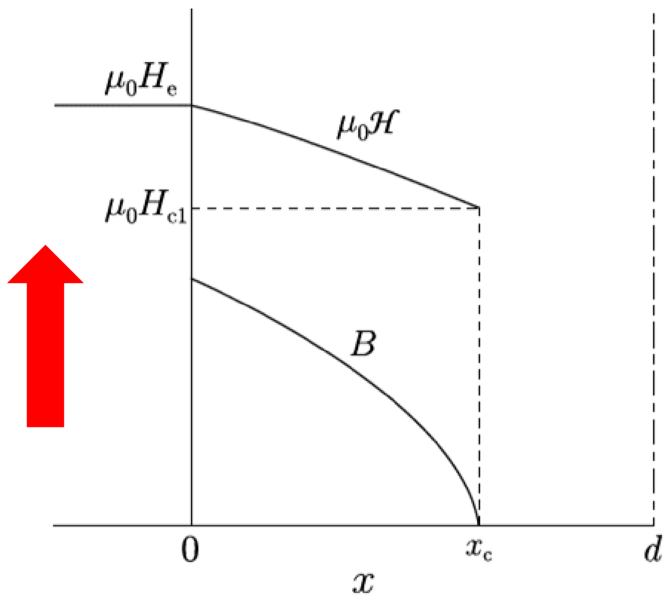

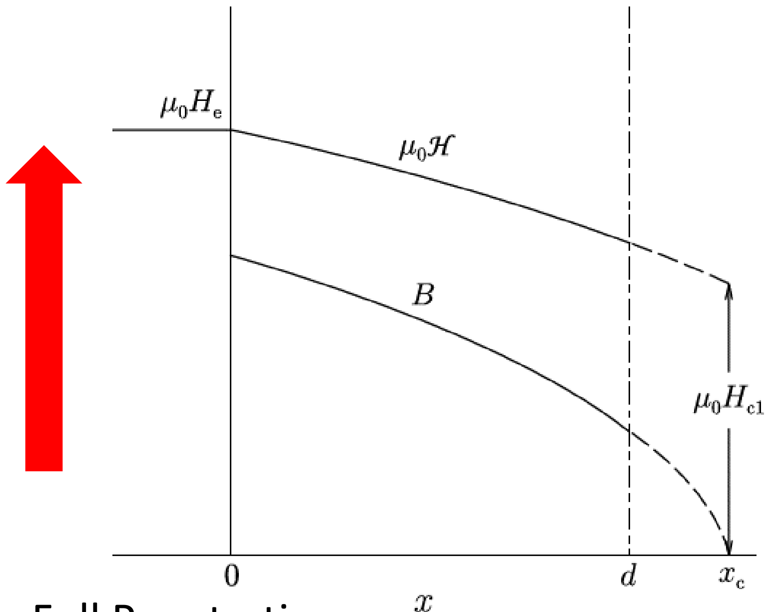

Full Penetration

Decreasing Field

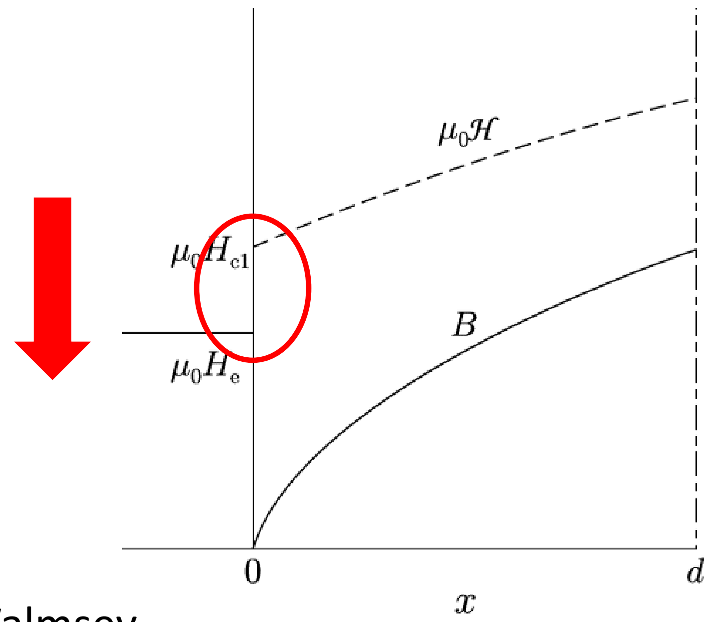

Walmsey

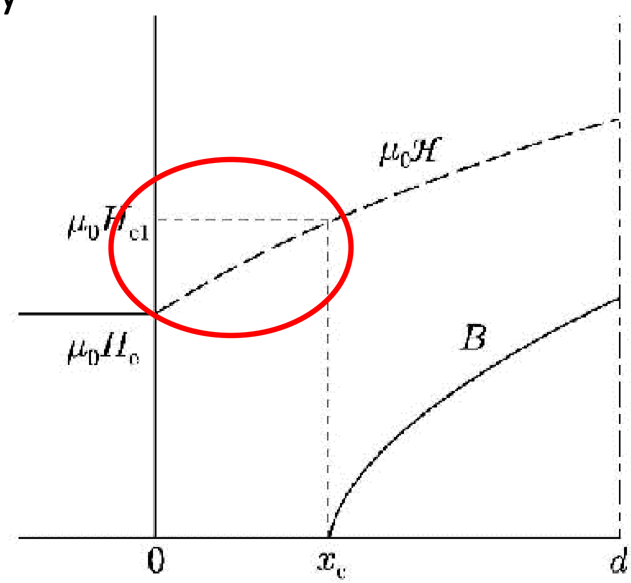

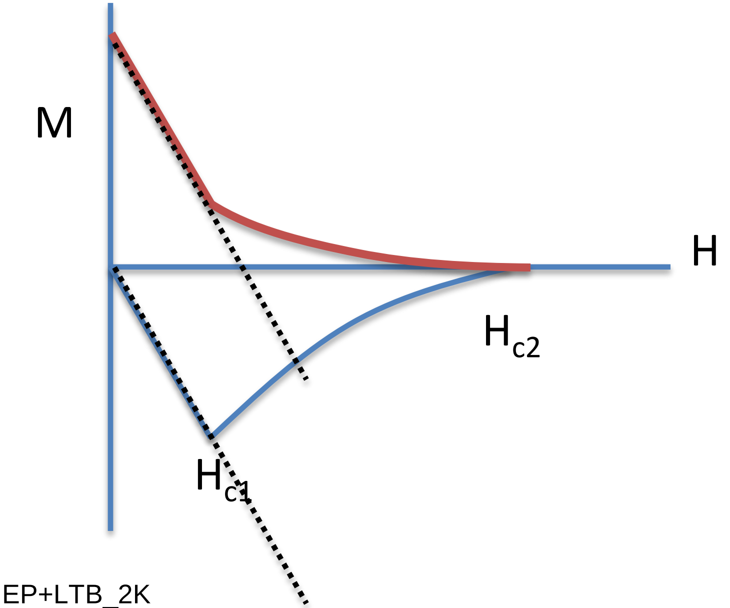

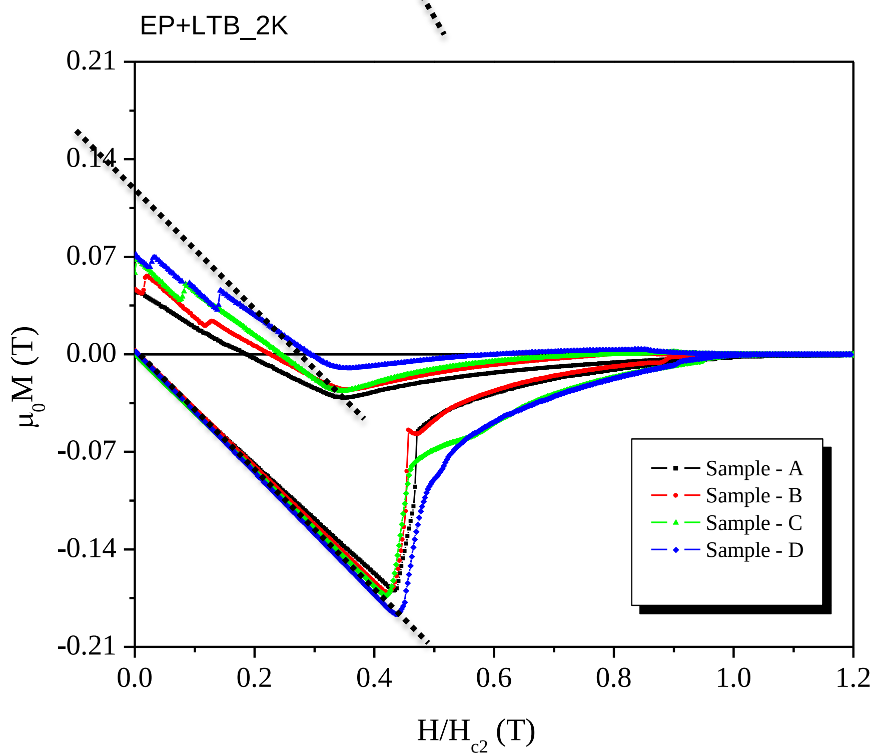

Matsushita Flux line discharge by diamagnetism

Matsushita derived an expression for the magnetization on the basis of a semi-microscopic model where the superconductor is considered as a multi-layered structure composed of ideal superconducting layers and thinner pinning layers.

Flux Pinning in Superconductors, Springer

The force balance equation

$$dH/dx = \mp J_c(B) = \mp F_p(B)/B \qquad for \quad H > H_{c1}$$

$$dH/dx = \mp(a - bH) \qquad for \quad 0 \le H \le H_{c1}$$

valid in the remnant state where trapped fluxoids exist

Relation between B and H

$$B(H) = \mu_0 H + M(H) = \mu_0 H - \mu_0 H_{c1}\left[1 - \left(\frac{H - H_{c1}}{H_{c2} - H_{c1}}\right)^{\beta}\right] \qquad \beta = \frac{\chi_{c2}}{\mu_0}\left(\frac{H_{c2}}{H_{c1}} - 1\right) \qquad \chi_{c2} = (dM/dH)_{H_{c2}}$$

Kes *et al.*, 1973 *J. of Low Temp. Phys.* **10** 759

Pinning force density

$$F_p(B) = \alpha\left(\frac{B}{B_{c2}}\right)^{\gamma}\left(1 - \frac{B}{B_{c2}}\right)^{\delta}$$

Campbell A M and Evetts J E 1972 *Advances is Phys.* **21** 199

Doing some math for long hollow cylinder of $R_{out} \le r \le R_{in}$

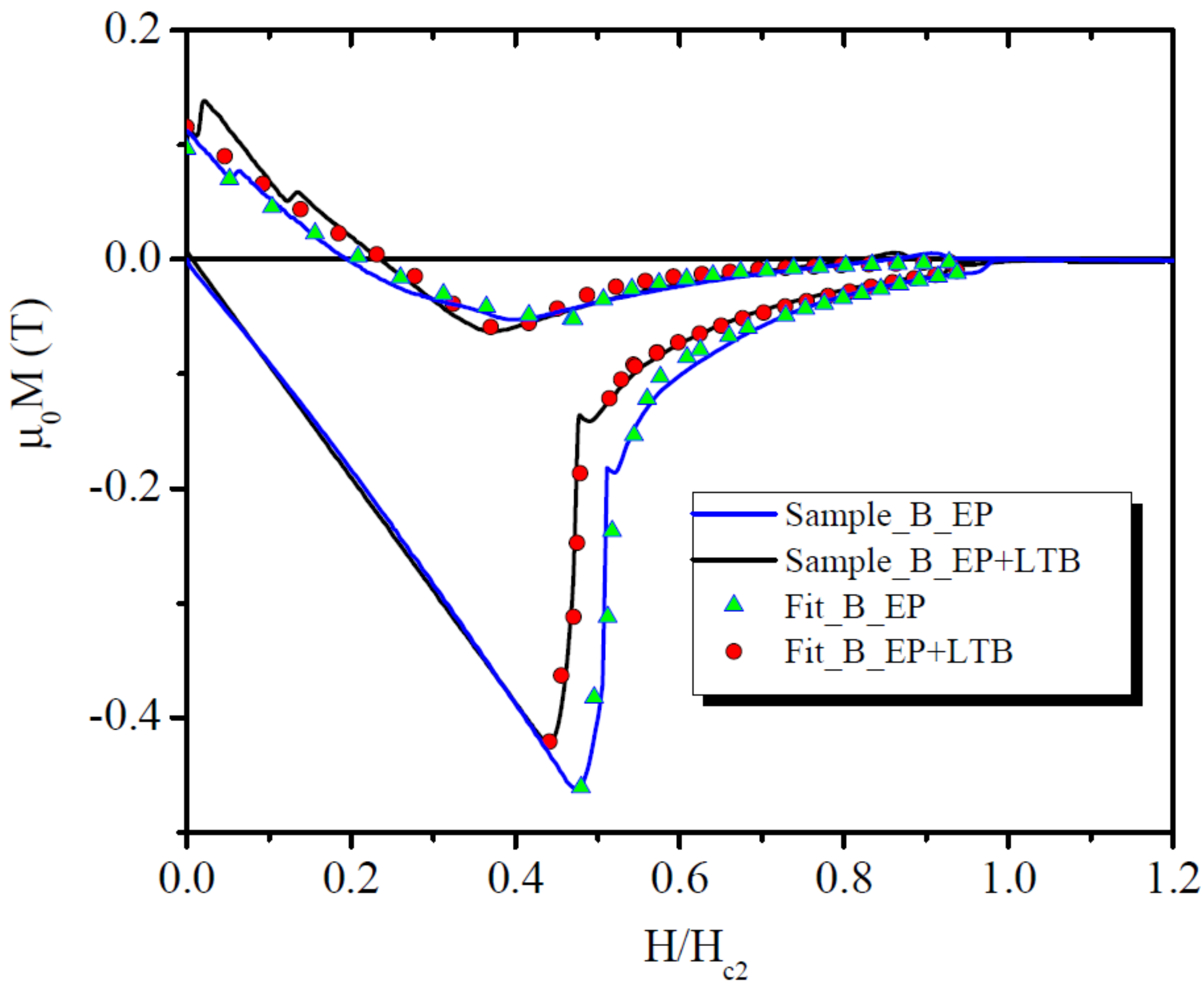

M $\quad$ c1 $\quad]^{-\delta} \; dH$ $\quad$ 2

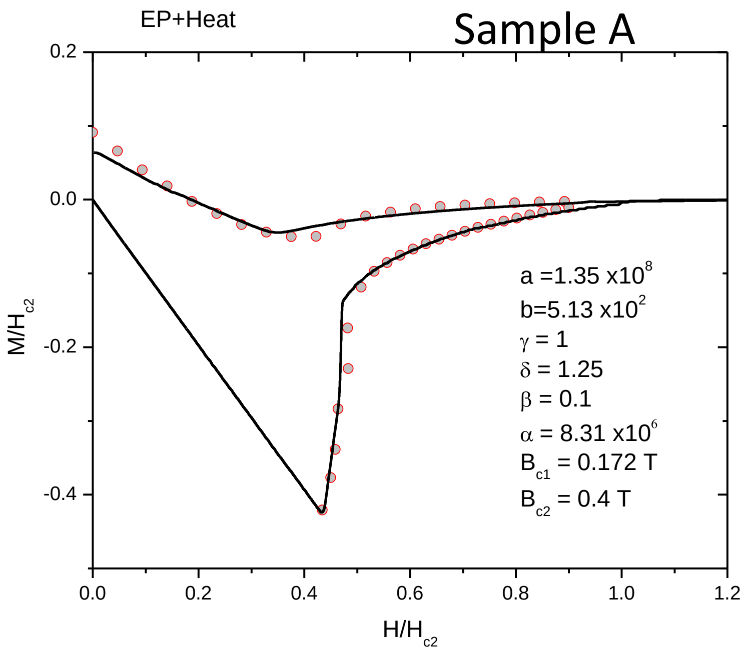
Sample A
EP+Heat
0.2
0.0
-0.2
-0.4
M/H_c2
0.0
0.2
0.4
0.6
0.8
1.0
1.2
H/H_c2
a =1.35 x10^8
b=5.13 x10^2
γ = 1
δ = 1.25
β = 0.1
α = 8.31 x10^6
B_c1 = 0.172 T
B_c2 = 0.4 T

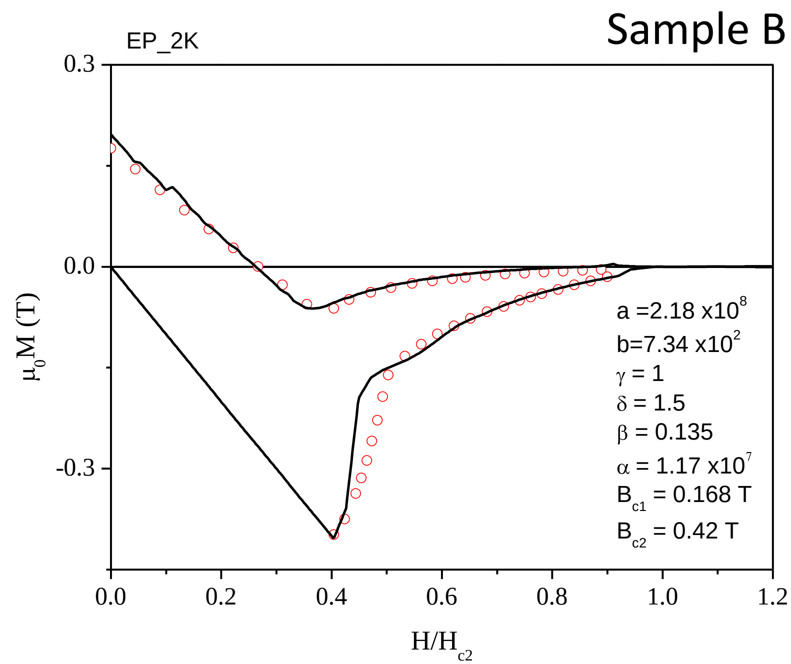
Sample B
EP_2K
0.3
0.0
-0.3
μ_0M (T)
0.0
0.2
0.4
0.6
0.8
1.0
1.2
H/H_c2
a =2.18 x10^8
b=7.34 x10^2
γ = 1
δ = 1.5
β = 0.135
α = 1.17 x10^7
B_c1 = 0.168 T
B_c2 = 0.42 T

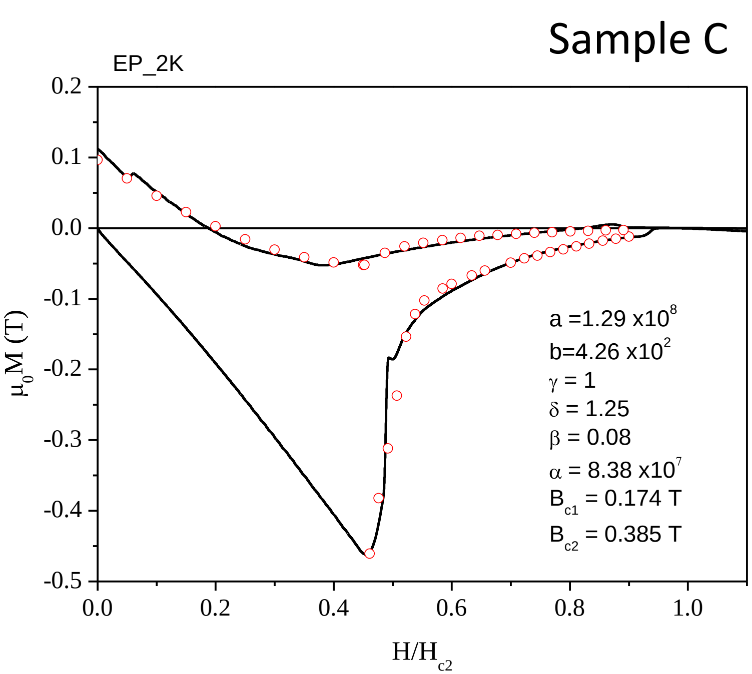
Sample C
EP_2K
0.2
0.1
0.0
-0.1
-0.2
-0.3
-0.4
-0.5
μ_0M (T)
0.0
0.2
0.4
0.6
0.8
1.0
H/H_c2
a =1.29 x10^8
b=4.26 x10^2
γ = 1
δ = 1.25
β = 0.08
α = 8.38 x10^7
B_c1 = 0.174 T
B_c2 = 0.385 T

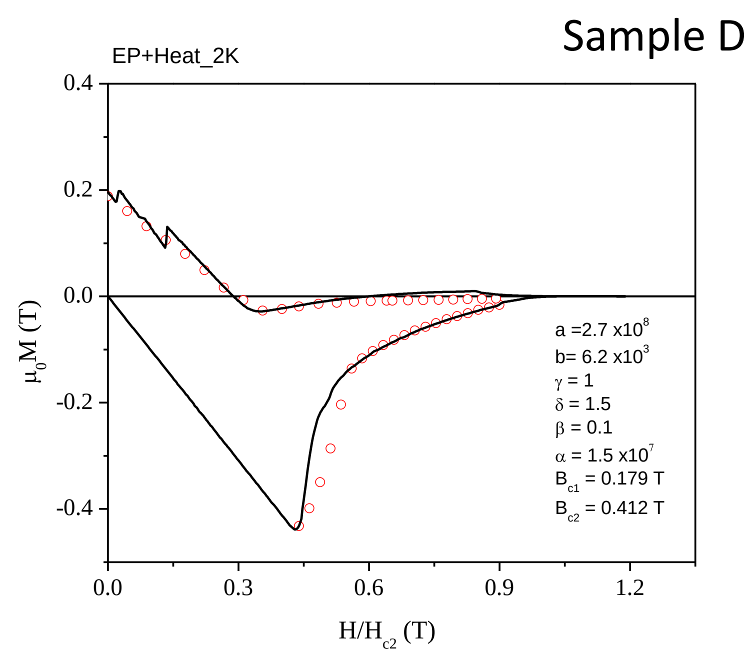
Sample D
EP+Heat_2K
0.4
0.2
0.0
-0.2
-0.4
μ_0M (T)
0.0
0.3
0.6
0.9
1.2
H/H_c2 (T)
a =2.7 x10^8
b= 6.2 x10^3
γ = 1
δ = 1.5
β = 0.1
α = 1.5 x10^7
B_c1 = 0.179 T
B_c2 = 0.412 T

Fitting Parameters

Fitting Parameter	Sample A		Sample B		Sample C		Sample D	
	EP	EP+Heat	EP	EP+Heat	EP	EP+Heat	EP	EP+Heat
a (A/m^2)	1.6×10^8	1.35×10^8	1.29×10^8	1.37×10^8	2.18×10^8	2.18×10^8	2.8×10^8	2.7×10^8
b	5.13×10^2	5.13×10^2	4.26×10^2	4.31×10^2	7.34×10^2	7.34×10^2	6.3×10^2	6.2×10^2
α (N/m^3)	4.38×10^6	8.31×10^6	8.38×10^6	8.08×10^6	1.17×10^7	1.28×10^7	1.4×10^7	1.5×10^7
β	0.1	0.1	0.08	0.08	0.135	0.1	0.1	0.1
γ	1	1	1	1	1	1	0.75	1
δ	1.25	1.25	1.25	1.25	1.5	1.5	1.5	1.5

Effect of Surface Treatment and Heat Treatment on M

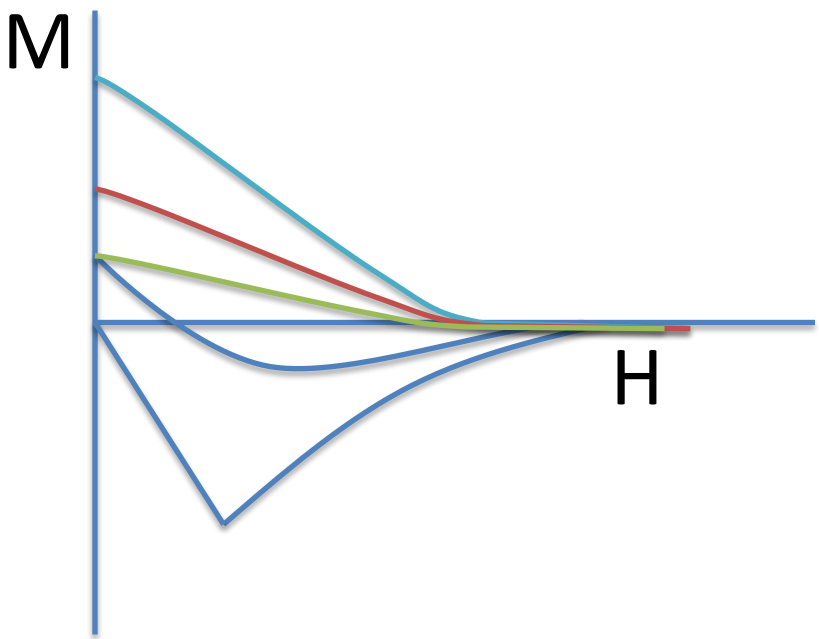

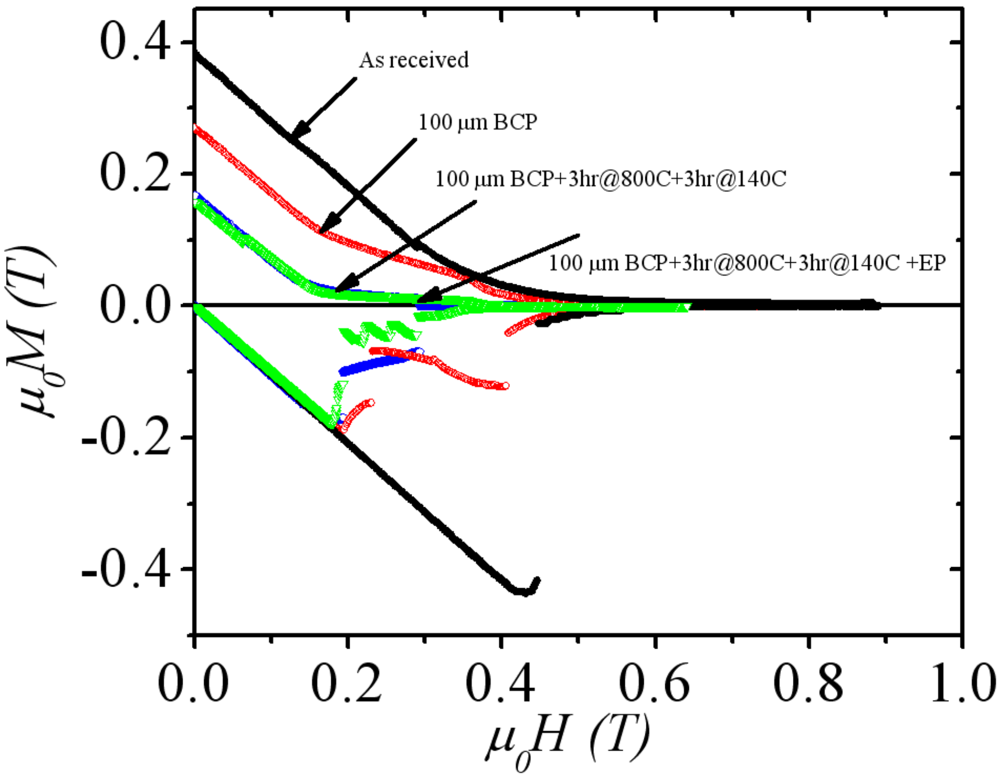

Hysteresis decreases → Reduced pinning → Increase Q_0

Critical Current

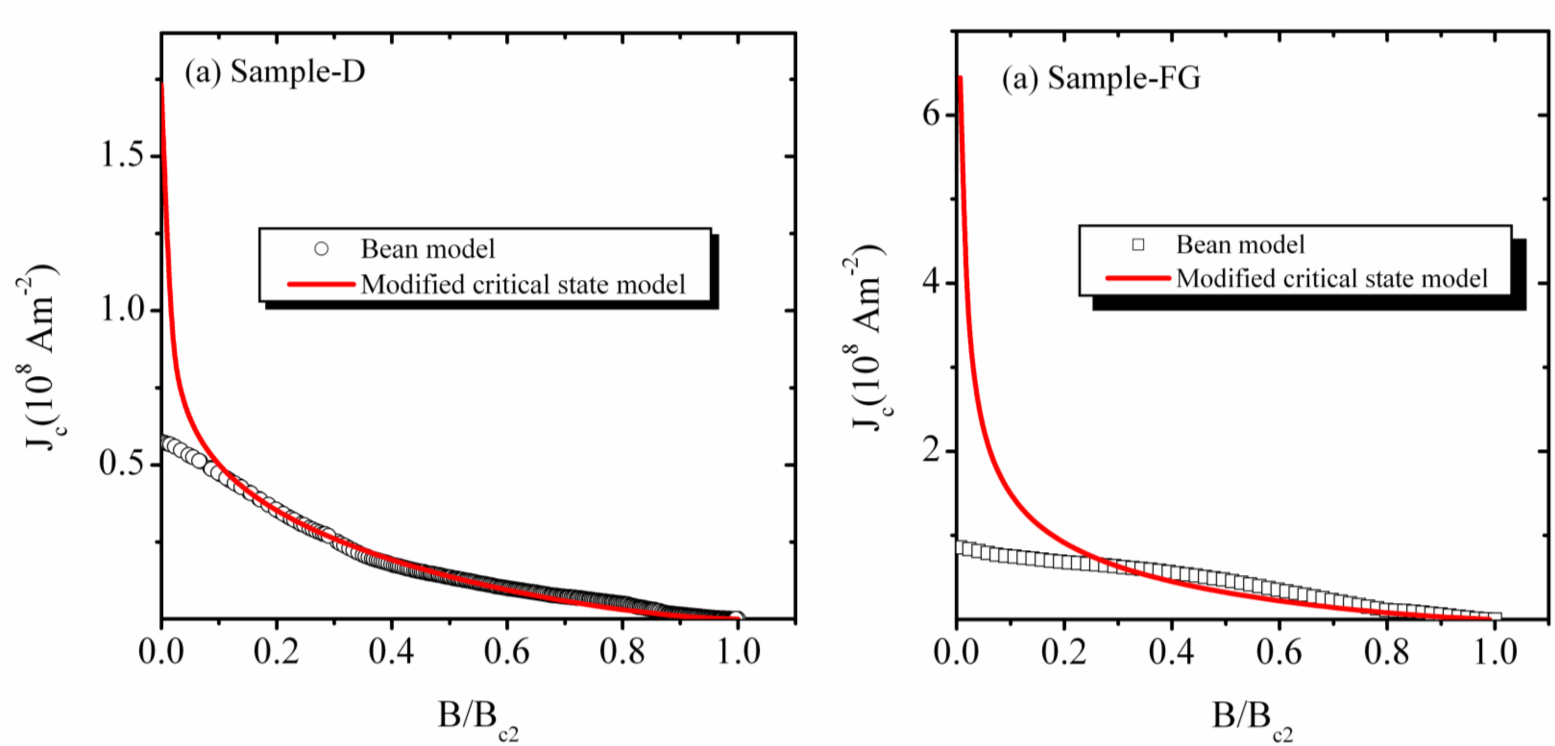

Bean's model underestimates J_c at low magnetic flux densities compared to other critical state models which better describe magnetization data.

Similar conclusion was obtained from the analysis of magnetization data for NbTi[1]

[1]Douine B, Leveque J and Mezani S 2010 *IEEE Trans. on Appl. Supercond.* **20 (2)** 82

Magnetization of FG Sample

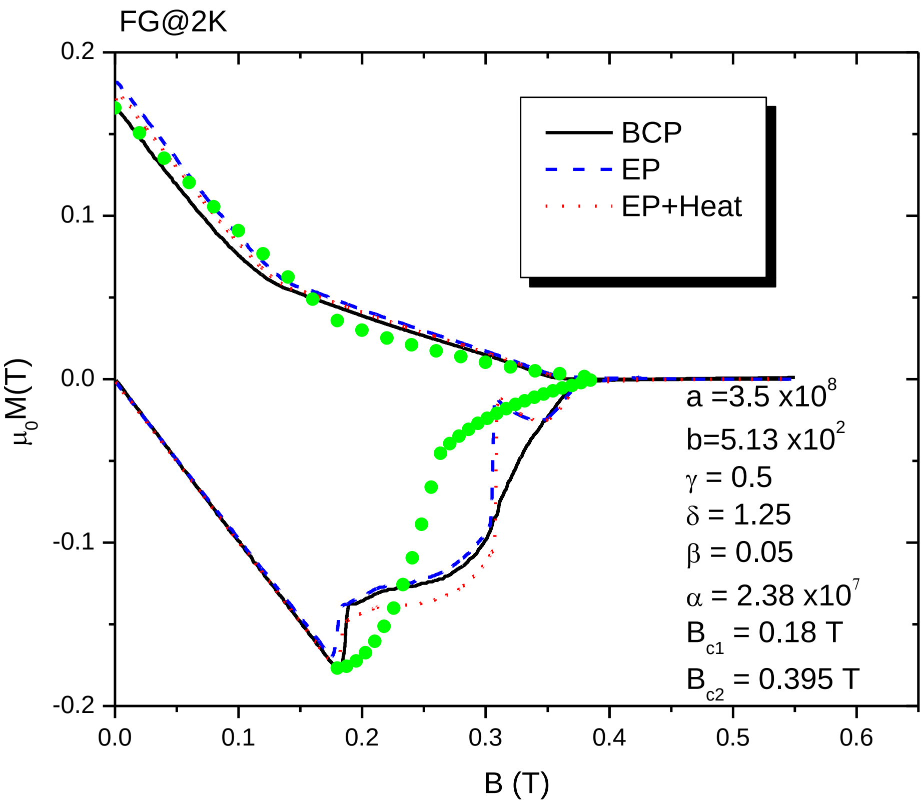

Strange "belly" shaped couldn't not reproduce in calculations, sample was cut inspected magneto-optical imaging (NHMFL) and planned to do magnetization measurement in commercial magnetometer.

Anatolii Polyanskii, NHMFL

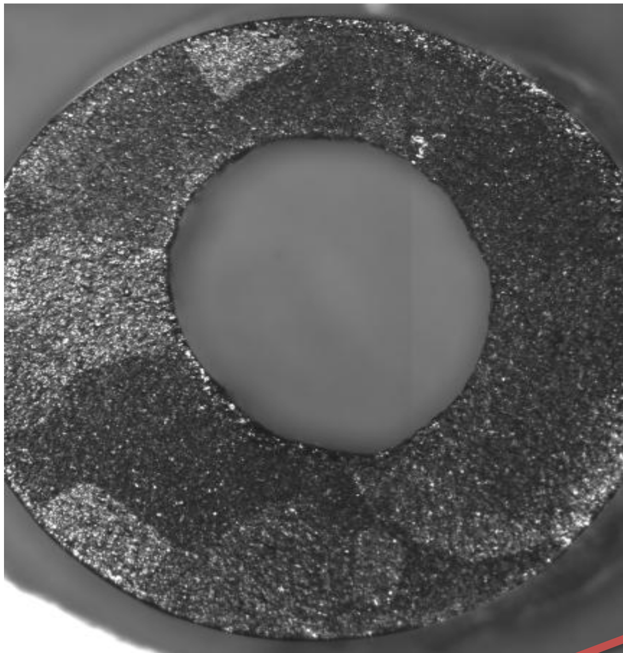

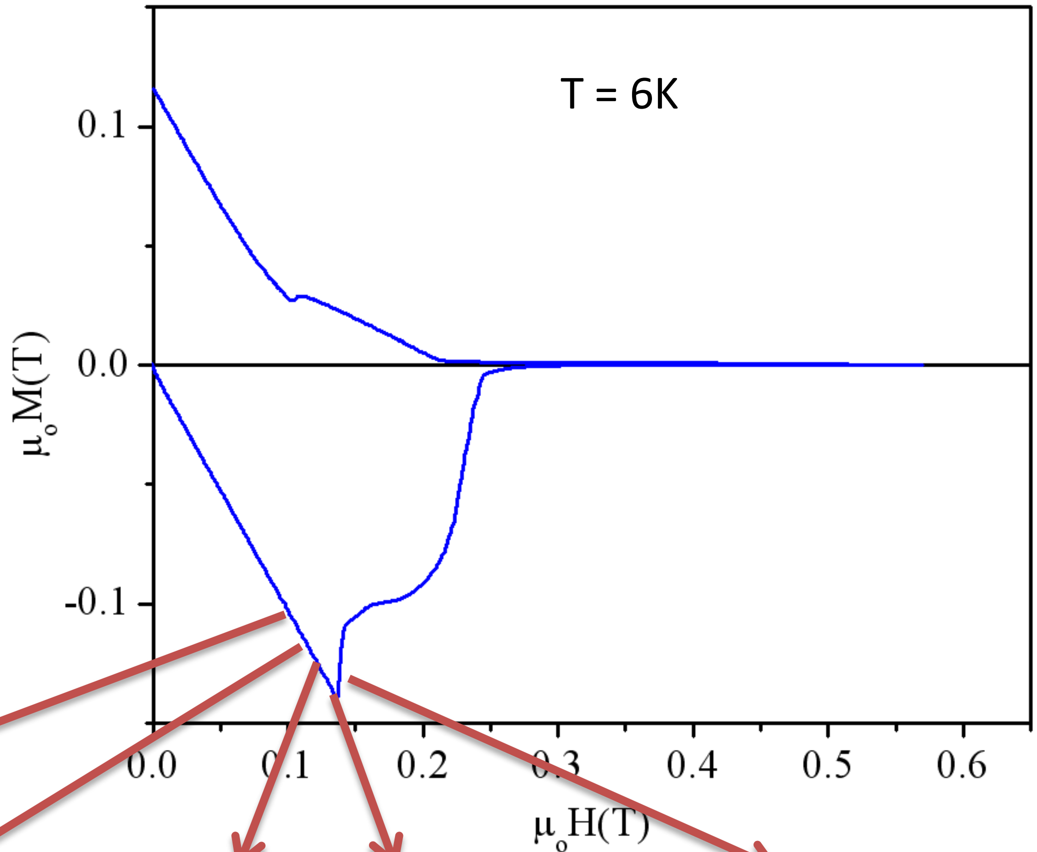

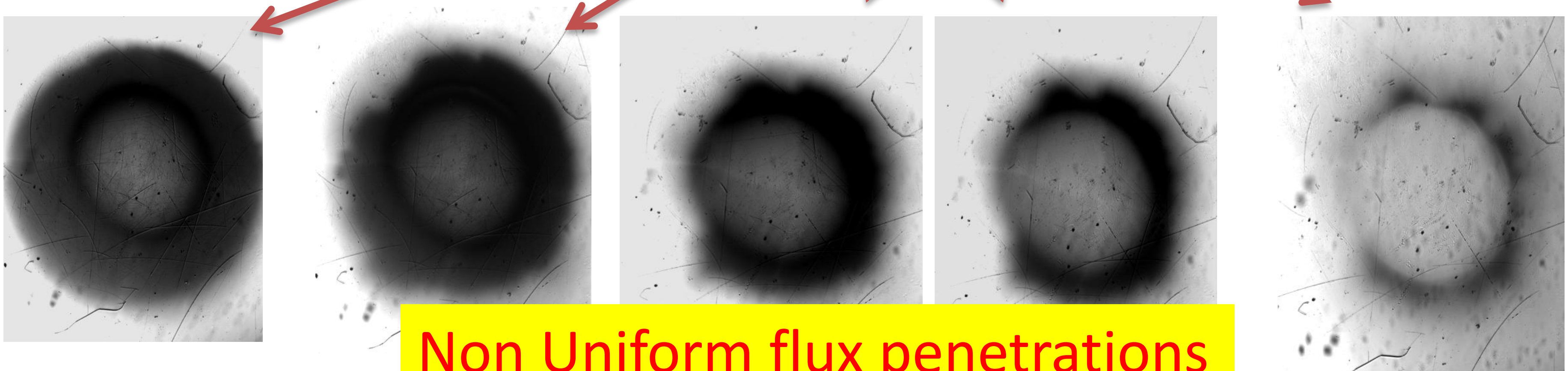

Non Uniform flux penetrations

80 mT

100 mT

120 mT

124 mT

140 mT

Conclusions

✍ Even though the LG samples have different RRR values, the magnetic properties of these large grain samples do not depend on the bulk impurity concentrations.

✍ Using the modified critical state model by Matsushita the irreversible magnetization was calculated showing good agreement with the experimental data.

✍ The calculated J_c and F_p of LG samples (A-D) are lower than the FG, as expected because of the fewer grain boundaries.

✍ Large-grain Nb would be less efficient in pinning magnetic flux during the cavity cool-down, compared to fine-grain Nb, because of the lower J_c. This would result in reduced RF losses (higher Q_0-value) for large-grain cavities.

RF Measurements

Coax-cavity cavity

T. Junginger

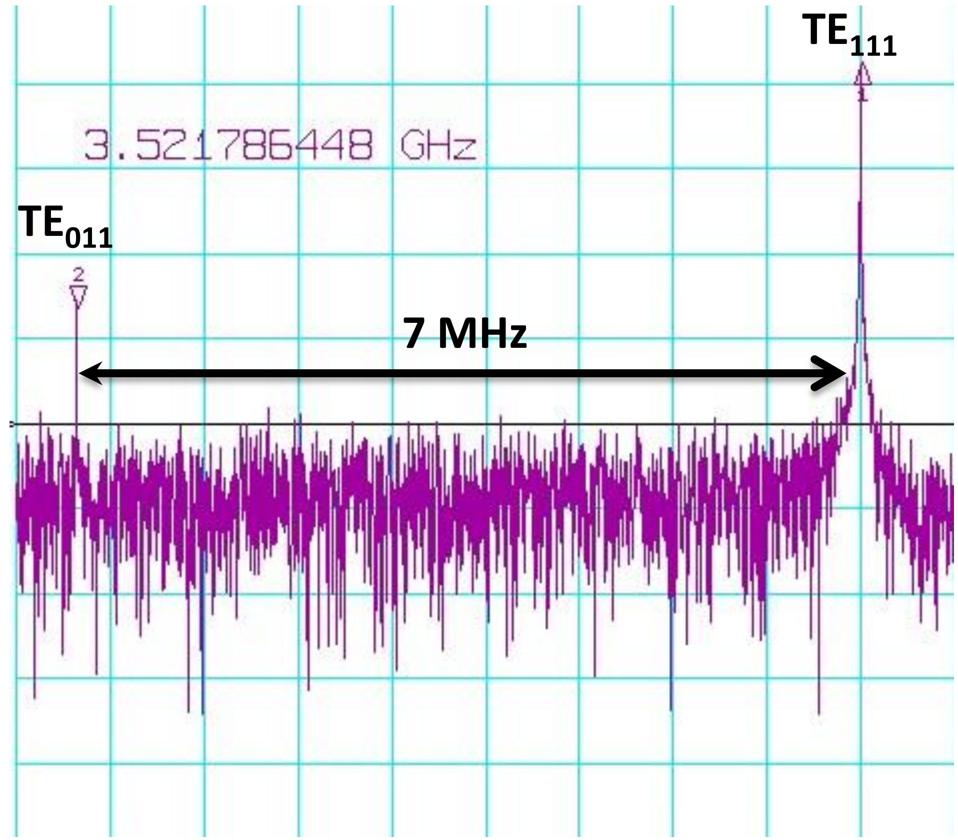

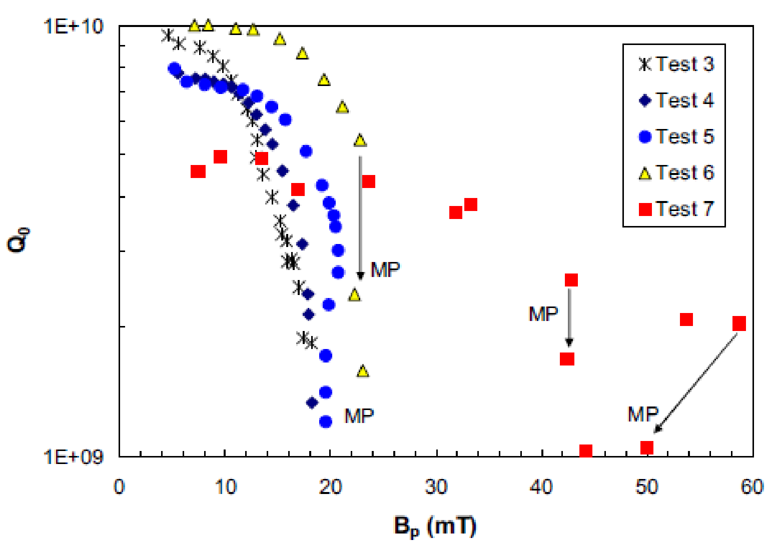

Ciovati et al., SRF 2007

Coax-cavity cavity

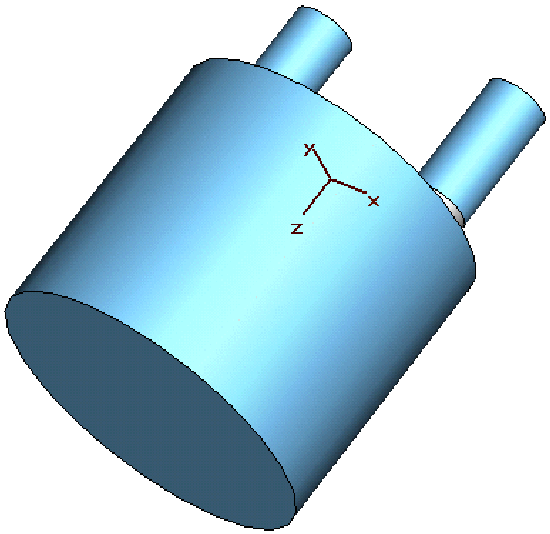

Original flat base plate

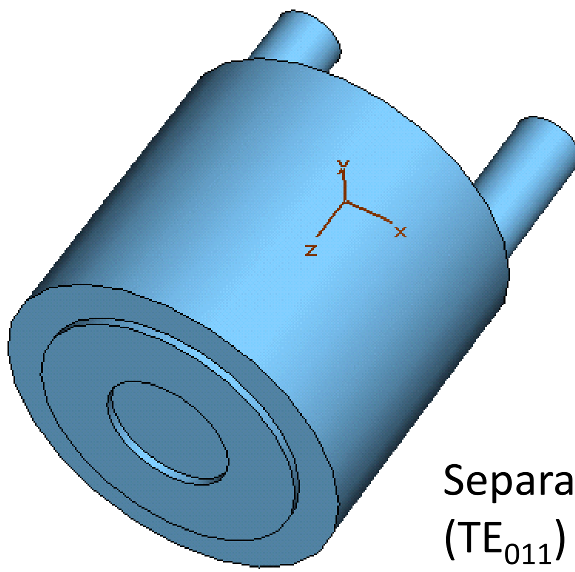

With modified base plate

sample

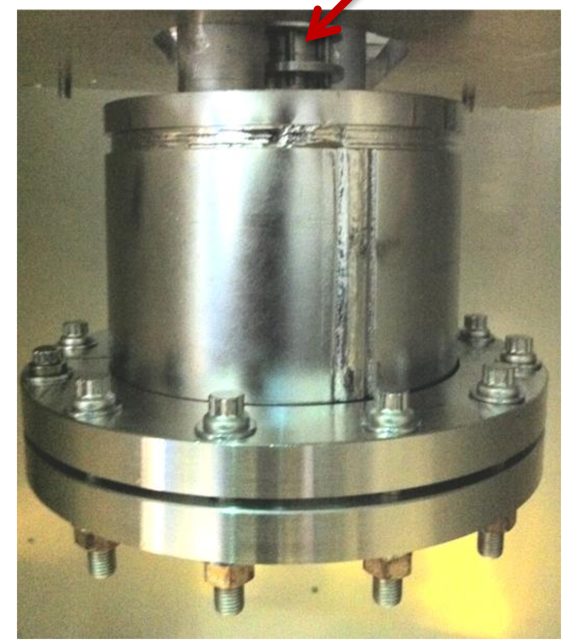

Separation between the operating mode (TE_{011}) and the neighbouring TM_{111} mode from the initial 7 MHz to about 32 MHz.

RF Properties-Coax Cavity

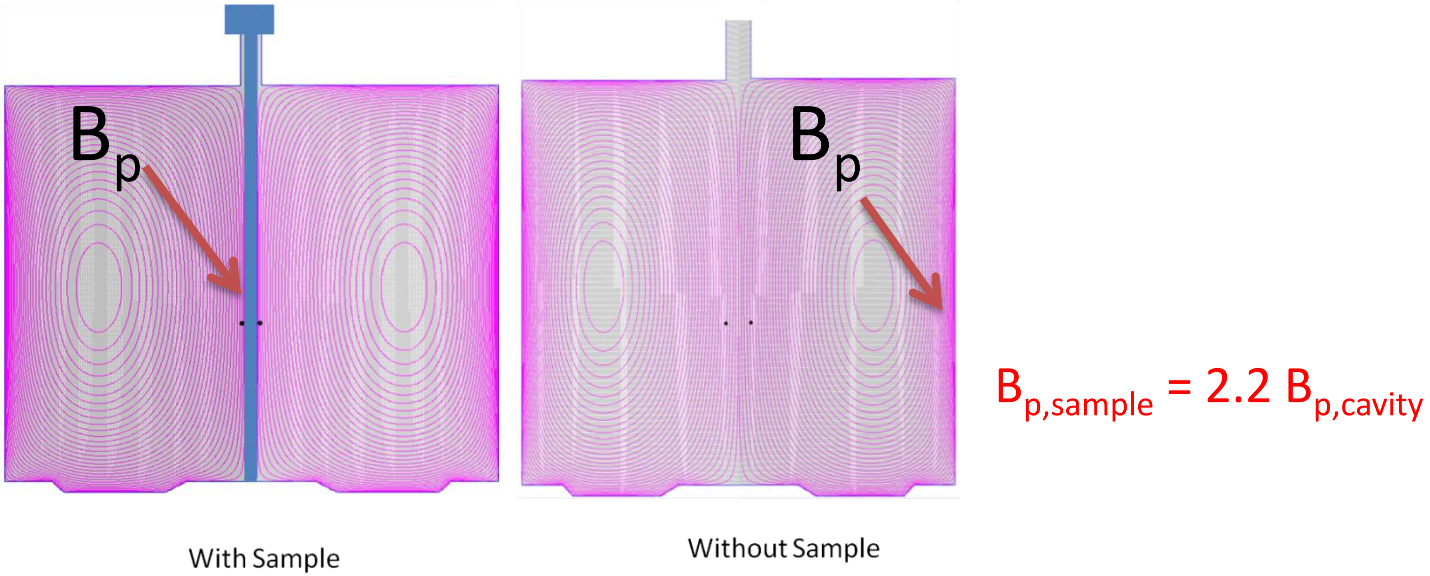

field distribution in cavity

Parameters	Empty	w. sample
Resonant frequency (GHz)	3.501	3.856
$Bp/\sqrt{U}$ (mT/J)	62.7	114.2
Geometric factor (G)	779.6 Ω	532.2 Ω

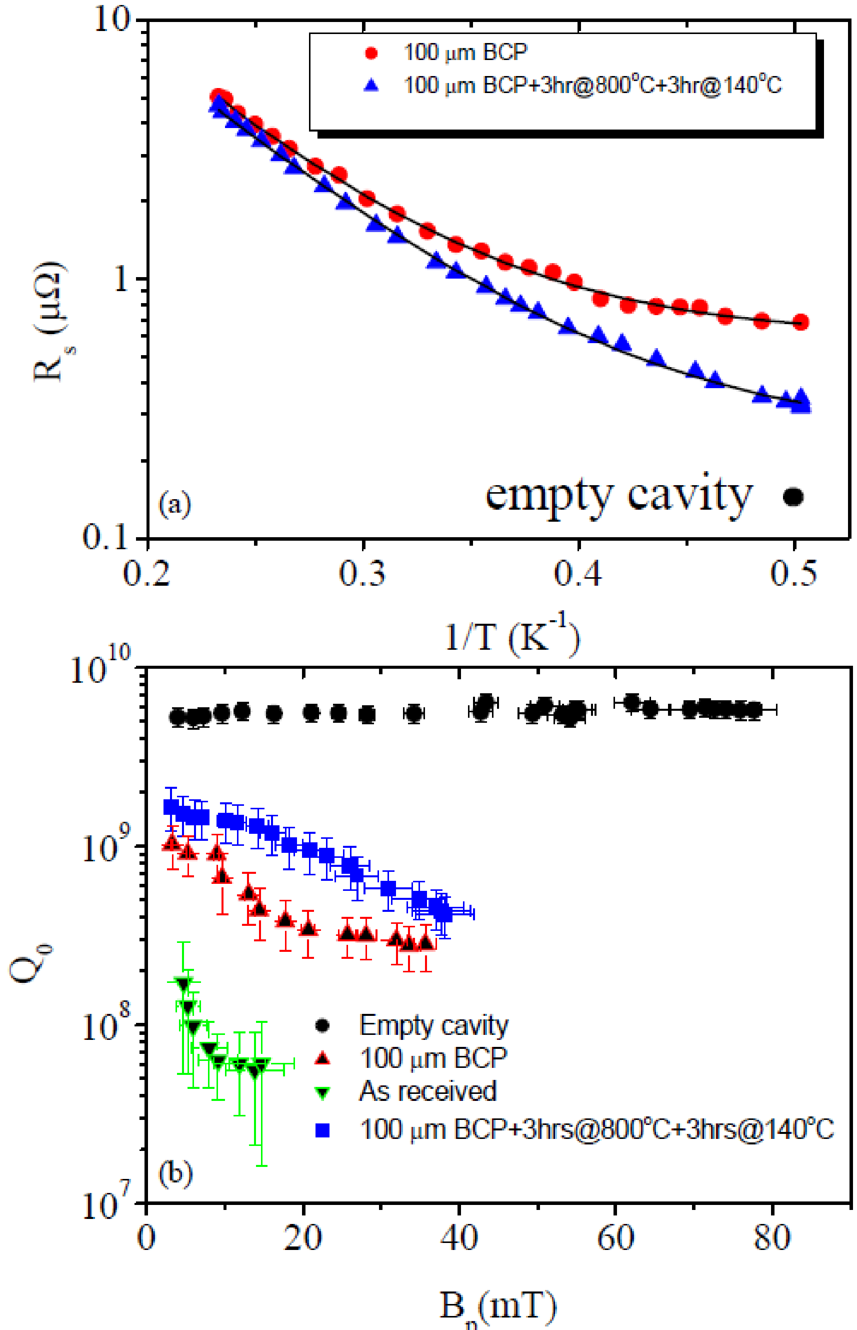

$R_s = R_{BCS}+R_{res}$

$$R_{BCS} = 2\times10^{-4}\left(\frac{f}{1.5\times10^{9}}\right)^{2}\frac{e^{-17.67/T}}{T}(\Omega)$$

R_{res} = 609±24 nΩ and 254±13 nΩ and Δ/K_BT_c = 1.83±0.02 and 1.73±0.07 after BCP and after additional heat treatment

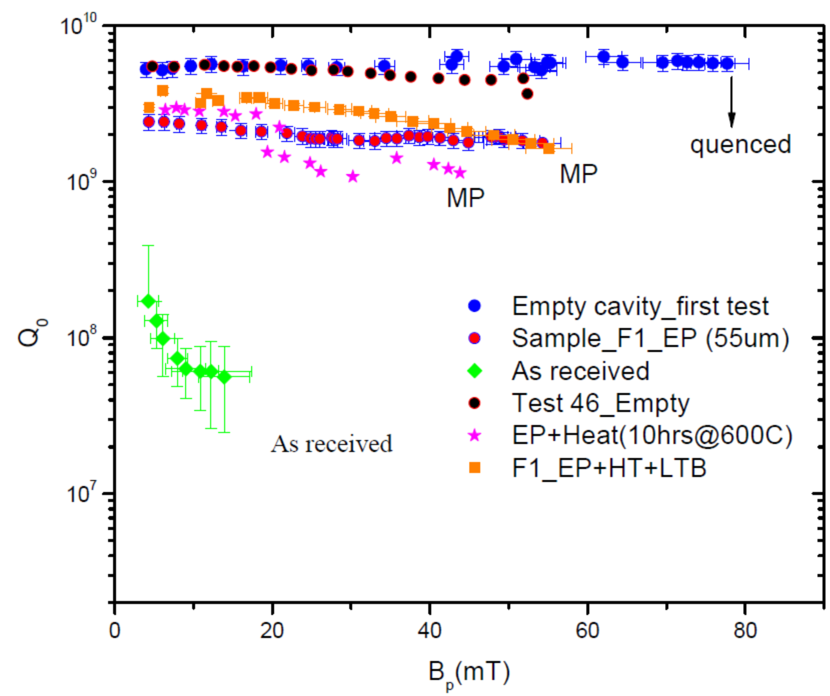

Dhakal et al., SRF 2011

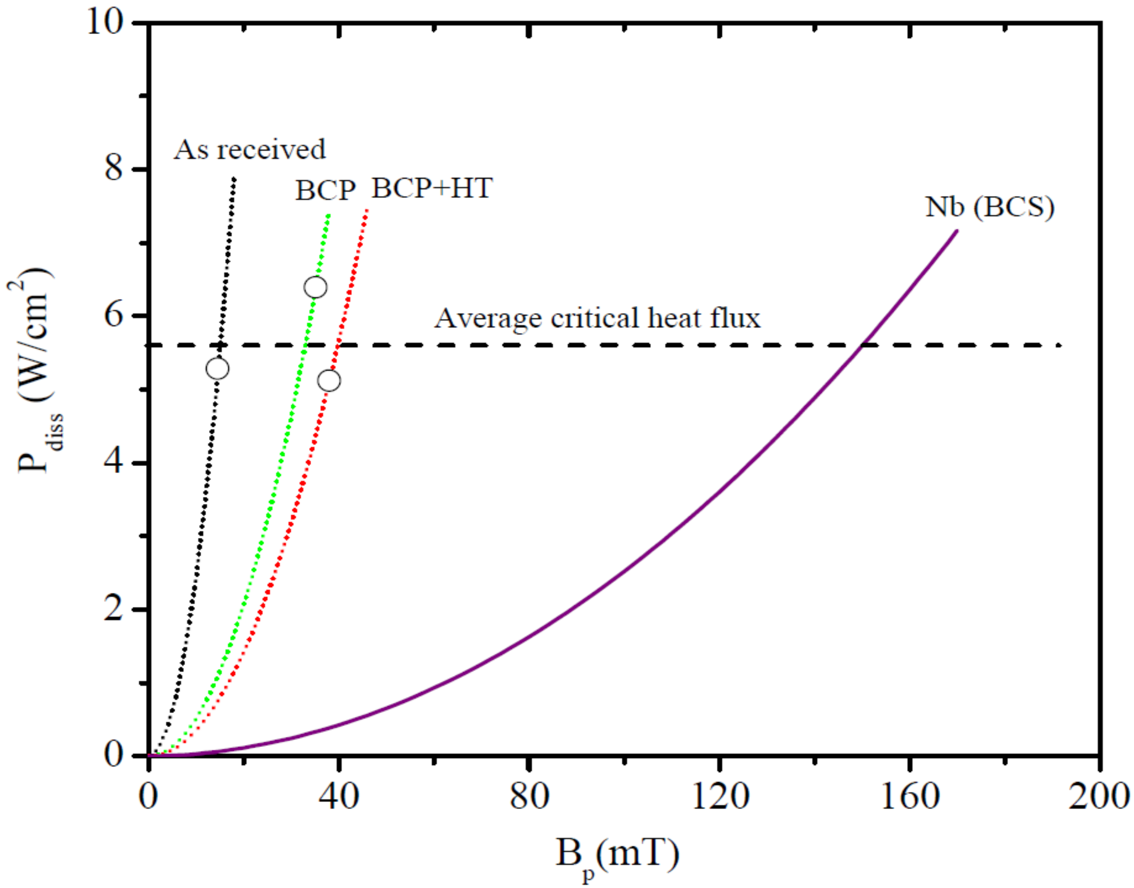

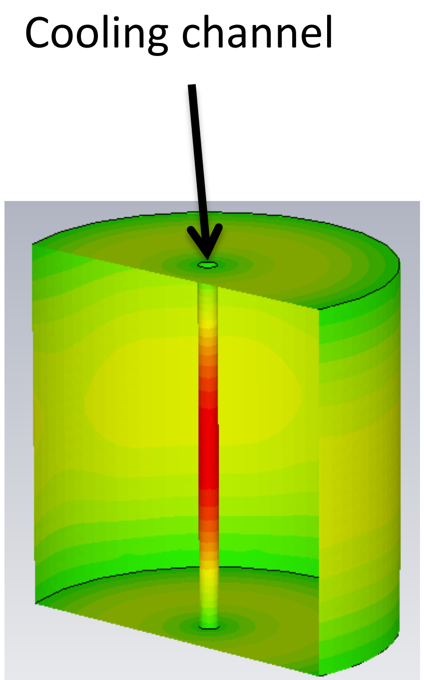

Highest field limited by critical heat flux through the cooling channel

System capable of measuring RF properties of any superconducting samples.

Conclusions

✍ Even though the LG samples have different RRR values, the magnetic properties of these large grain samples do not depend on the bulk impurity concentrations.

✍ Using the modified critical state model by Matsushita the irreversible magnetization was calculated showing good agreement with the experimental data.

✍The calculated J_c and F_p of LG samples (A-D) are lower than the FG, as expected because of the fewer grain boundaries.

✍ Large-grain Nb would be less efficient in pinning magnetic flux during the cavity cool-down, compared to fine-grain Nb, because of the lower J_c. This would result in reduced RF losses (higher Q_0-value) for large-grain cavities.

✍ RF measurement on TE_{011} cavity shows the reduction of surface resistance and hence the increase in quality factor due to the chemical and heat treatment, however maximum peak magnetic field is limited due to the critical heat flux of the niobium rods.

Acknowledgement

G. Ciovati
A. Dhavele
M. Marrone
P. Kushnick

Thank You